JOURNAL OF MATERIALS SCIENCE 32 (1997) 3299 – 3304

Enhancing effect of Cl_2 atmosphere on transition aluminas transformation

E. M. LOPASSO, J. J. ANDRADE GAMBOA, J. M. ASTIGUETA, D. M. PASQUEVICH
Centro Atómico Bariloche, Comisión Nacional de Energía Atómica, (8400) S.C. de Bariloche. Río Negro, Argentina

In the present study we examine the changes in phase composition and microstructure undergone by solids after thermal treatments performed on transition aluminas in chlorine and air atmospheres. The thermal transformation to the stable α-Al_2O_3 was faster for the chlorine-heated samples than for the air-heated ones, and for chlorinated samples single crystals of α-Al_2O_3 were observed. We propose a mechanism by which $AlCl_3$(g) formation allowed vapour mass transport that contributed to the growth of crystals of α-Al_2O_3. Hydroxyls contained in transition aluminas could enhance gaseous transport and could also react with chlorine molecules. The subsequent α-Al_2O_3 crystallization would be assisted by water vapour.

1. Introduction

Aluminium oxide (Al_2O_3) has a unique stable crystalline phase, named corundum or α-phase, which can be formed by calcination of aluminium hydroxides [1, 2]. Depending on time and temperature of the calcination, other intermediate phases of Al_2O_3, known as transition aluminas, can also be obtained [3–7]. Transition aluminas are metastable and structurally similar phases, and have structural hydroxyls (OH) which is one of their most important common features [2, 3, 9, 11]. The transformation of transition aluminas to α-phase involves a dehydration process from internal OH layers and an increasing ordering of the defect spinel lattice. Although it is not well established, the transformation could involve a collapse phenomenon in their layered structure [3, 9, 11].

Several factors affect the transformation of transition aluminas. Calcination in air to α-Al_2O_3 involves a sequence that is precursor dependent [4, 8, 9]. For instance, in the case of well-crystallized boehmite (AlOOH), the calcination leads to the $\gamma-\delta-\theta-\alpha$ sequence as temperature increases [9]. The phase transformation of transition aluminas is also affected by the presence of impurities and the heating atmosphere [5, 7, 10–16]. The study of the effect of the atmosphere on the transformation was mainly focused on oxygen and water vapour, which are known to accelerate transition aluminas transformation [10, 11].

Previous studies have shown the accelerating effect of chlorine atmosphere on tetragonal (metastable) to monoclinic (stable) transformation in ZrO_2 [18] and anatase (metastable) to rutile (stable) transformation in TiO_2 [19]. The enhancing effect of chlorine atmosphere on the transformation of transition aluminas to α-phase was also reported [17]. The aim of the present work is to study the effect of chlorine on the transformation of transition aluminas, and to correlate it with the growth of single crystals of α-Al_2O_3.

2. Experimental procedure

Starting materials were prepared by heating well crystallized boehmite [17] in dry air in open quartz crucibles. Three batches, containing delta alumina as a component, were obtained by performing the following treatments: (1) 900 °C for 11 h (Batch δ900, containing only delta alumina); (2) 950 °C for 11 h (Batch δ950, containing a mixture of delta and theta aluminas); and (3) 1000 °C for 20 h (Batch δ1000, containing a mixture of delta and theta aluminas, with a minor amount of the stable alpha phase). Details of the preparation of these starting batches are given in Table I.

Each batch received subsequent heating at the same temperature at which it was prepared. Thermal treatments were performed during different time intervals, in air in open quartz crucibles, and in chlorine in sealed quartz crucibles. Sealed samples were encapsulated with pure Cl_2 (99.8%) at room temperature. Assuming chlorine as an ideal gas we estimated the pressure of encapsulation as the one leading to a total pressure of 1.013×10^5 Pa at each treatment temperature. Samples heated in chlorine received subsequent thermal treatments in open air. After heating, samples were quenched at room temperature and X-ray powder diffraction analyses (XRD*, CuK_α Ni filtered radiation) were performed to identify the resultant phases. The microstructural changes associated to each treatment were characterized using Scanning Electron

* PW 1300, Philips Electronic Instruments.

0022–2461

TABLE I Thermal treatments on boehmite to obtain starting batches, and phases present in them

Batch	Obtained by firing of boehmite	Detected phases
δ900[a]	at 900 °C during 11 h	δ
δ950[b]	at 950 °C during 11 h	δ + θ
δ1000[c]	at 1000 °C during 20 h	δ + θ + (α)[d]

[a] XRD diagram shown in Fig. 1a.
[b] XRD diagram shown in Fig. 2a.
[c] XRD diagram shown in Fig. 3a.
[d] α-phase present in a small amount.

TABLE II Thermal treatments performed on starting batches

Run	Starting batch	Thermal treatment temperature (°C)	Thermal treatment (time and atmosphere)	Detected phases
1	δ900	900	15 h in air	δ
2	δ900	900	30 h in air	δ
3[a]	δ900	900	60 h in air	δ + θ
4[a]	δ900	900	15 h in chlorine	δ + θ + α
5[a]	δ900	900	30 h in chlorine	δ + θ + α
6	δ900	900	15 h in Cl_2 + 35 h in air	δ + θ + α
7	δ900	900	30 h in Cl_2 + 20 h in air	δ + θ + α
8	δ950	950	15 h in air	δ + θ
9	δ950	950	30 h in air	δ + θ
10[b]	δ950	950	60 h in air	δ + θ
11[b]	δ950	950	15 h in chlorine	δ + θ + α
12[b]	δ950	950	30 h in chlorine	δ + θ + α
13	δ950	950	15 h in Cl_2 + 35 h in air	δ + θ + α
14	δ950	950	30 h in Cl_2 + 20 h in air	δ + θ + α
15	δ1000	1000	20 h in air	δ + θ + α[d]
16	δ1000	1000	40 h in air	δ + θ + α[d]
17[c]	δ1000	1000	60 h in air	δ + θ + α[d]
18[c]	δ1000	1000	20 h in chlorine	δ + θ + α
19[c]	δ1000	1000	40 h in chlorine	δ + θ + α
20	δ1000	1000	20 h in Cl_2 + 40 h in air	δ + θ + α
21	δ1000	1000	40 h in Cl_2 + 20 h in air	δ + θ + α

[a] XRD diagram shown in Fig. 1.
[b] XRD diagram shown in Fig. 2.
[c] XRD diagram shown in Fig. 3.
[d] α-phase present in a small amount.

Microscopy (SEM**). The details of all treatments are given in Table II, where the phases detected after each treatment are also indicated.

3. Results

3.1. Phase identification

The criteria used in the identification of transition aluminas are those proposed by Dauzat et al. [16]. Transition aluminas (γ, δ and θ phases) can be differentiated by analysing the XRD peaks between $2\Theta = 30.83^\circ$ and $2\Theta = 33.18^\circ$. The δ-phase is distinguished from the γ-phase by a peak at $2\Theta = 32.83^\circ$. The θ-phase differentiates from the other two by the peak at $2\Theta = 31.29^\circ$. Peaks at $2\Theta = 32.32^\circ$ and $2\Theta = 32.79^\circ$ for the γ and θ phases, respectively,

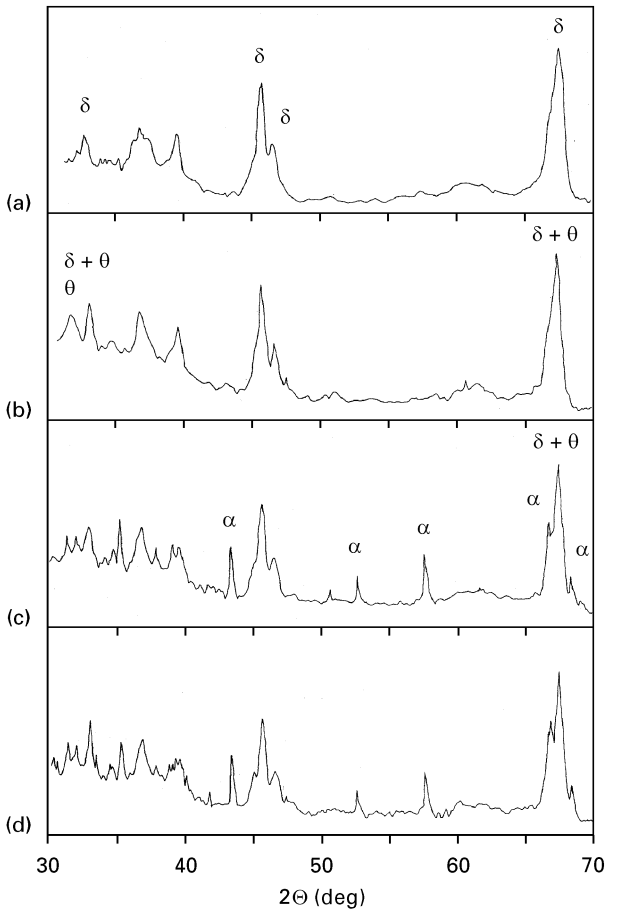

Figure 1 XRD diagrams obtained from (a) starting batch δ900, and after (b) 60 h at 900 °C in air, (c) 15 h at 900 °C in chlorine, and (d) 30 h at 900 °C in chlorine (heat treatments are runs 3–5 in Table II).

help also to identify the present phases in a mixture. Since the peaks at $2\Theta = 32.83^\circ$ for δ-phase and $2\Theta = 32.79^\circ$ for θ-phase are in fact overlapped, the $2\Theta = 31.29^\circ/2\Theta = 32.83^\circ$ ratio of integrated intensity peaks is used to determine the presence or absence of the δ-phase. When this ratio is lower than 0.6, the δ-phase coexists with the θ-phase [16]. The relative amount of α-phase to all transition aluminas can be estimated from the peaks in the range between $2\Theta = 65^\circ$ and $2\Theta = 70^\circ$. The peak at $2\Theta = 67.5^\circ$ is characteristic of all transition aluminas and is not present in the α-phase, and the peaks at $2\Theta = 66.6^\circ$ and $2\Theta = 68.2^\circ$ belong only to the α-phase. Their relative integrated intensities depend on the amount of α-phase relative to all transition aluminas in a given sample. Then, from the comparison between different XRD diagrams a qualitative estimation of the degree of transformation, relative to one of them, can be assessed.

Figs 1, 2 and 3 show the XRD patterns that correspond to the three batches. Each figure shows the diagrams before the thermal treatments (a), after the longest run in air (b), and after chlorine runs (c, d). The peaks belonging to each phase are indicated. All batches have common features: (1) The XRD pattern after the thermal treatment in air is similar to that of starting batch; (2) The XRD patterns after both

** SEM 515, Philips Electronic Instruments.

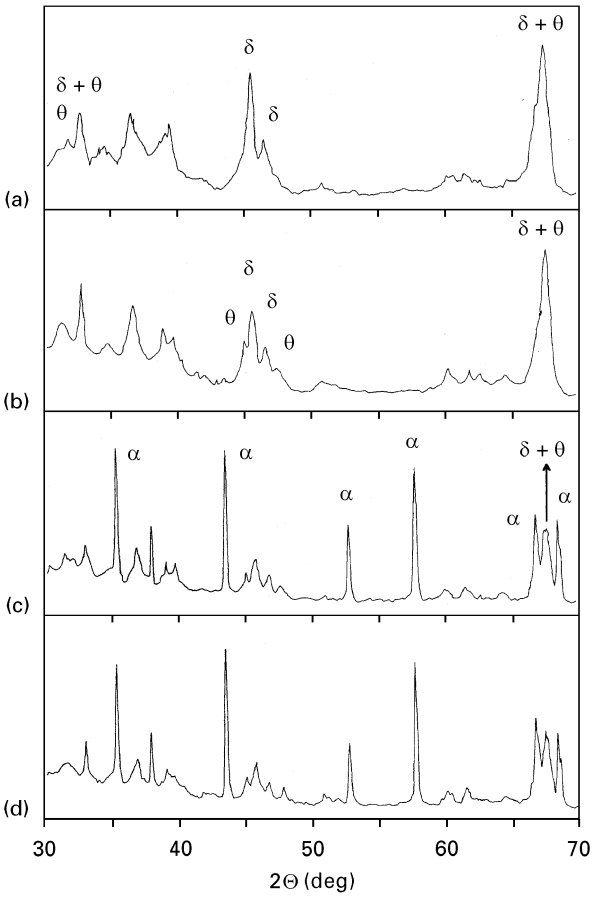

Figure 2 XRD diagrams obtained from (a) starting batch δ950, and after (b) 60 h at 950 °C in air, (c) 15 h at 950 °C in chlorine, and (d) 30 h at 950 °C in chlorine (Heat treatments are runs 10 – 12 in Table II)

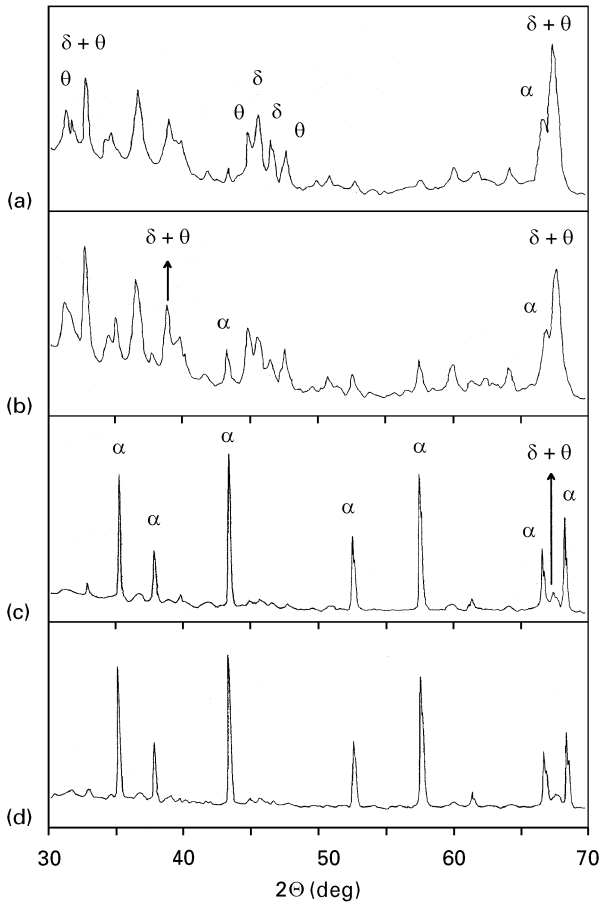

Figure 3 XRD diagrams obtained from (a) starting batch δ1000, and after (b) 60 h at 1000 °C in air, (c) 20 h at 1000 °C in chlorine, and (d) 40 h at 1000 °C in chlorine (Heat treatments are runs 17 – 19 in Table II).

thermal treatments in chlorine are equivalent; (3) The XRD patterns after treatments in chlorine show noticeable changes if compared to that of starting batch and involve the markedly apparition of α-phase. Also, it can be stated that the effect of chlorine is greater at higher temperatures and gives qualitatively more transformation from transition aluminas to α-phase. The XRD patterns for chlorinated samples that received further thermal treatments in air are not shown since in all cases no additional changes were observed.

3.2. SEM observations

The micrograph in Fig. 4 shows an oxide particle from starting batch δ1000 and a detail of its surface. Starting batches δ900 and δ950 showed identical characteristics. Particles of starting materials had an irregular surface formed by apparently agglomerated stepped blocks. Fig. 5 shows a particle corresponding to run 17 (Table II) which is representative of all thermal treatments in air. It can be observed that there were no microstructural changes.

After thermal treatments in chlorine, irrespective of temperature and duration of the heating, two types of oxide particles were observed: (1) one type was formed by an agglomeration of disc-shaped crystals (Figs 6 and 7); and (2) the other type exhibits disc-shaped crystals that grew over a matrix similar to that of the starting material (Fig. 8). Two main behaviours associated to the treatments in chlorine were observed: for

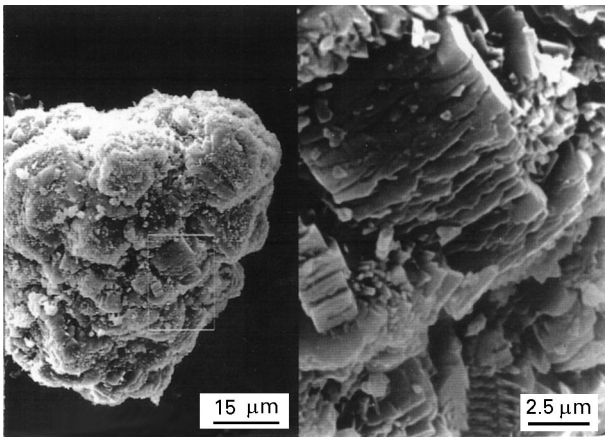

Figure 4 SEM micrograph of a particle (left) of the starting batch δ1000 and the surface detail (right) of marked zone (XRD diagram in Fig. 3a).

all runs, and for both types of oxide particles, the disc-shaped crystals had a narrow size distribution with a mean diameter of about 5 μm, and the global number of crystals (evaluated by simple visual inspection) is greater at higher temperatures.

4. Discussion

The phases present in starting batches δ900, δ950 and δ1000 are in agreement with the expected $\delta \rightarrow \theta \rightarrow \alpha$

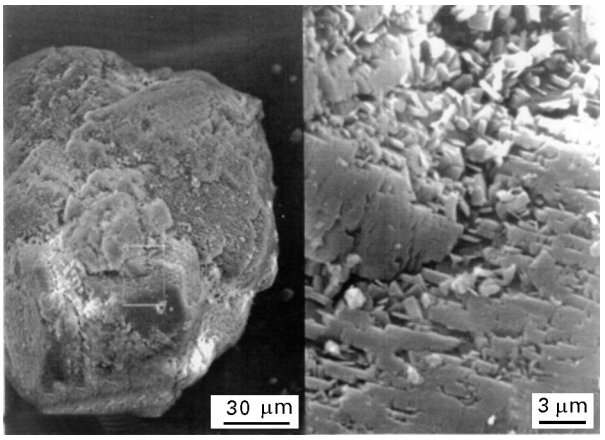

Figure 5 SEM micrograph of a particle of batch δ1000 (left) after heating in air at 1000 °C during 60 h (run 17 in Table II) and the surface detail (right) of marked zone (XRD diagram in Fig. 3b).

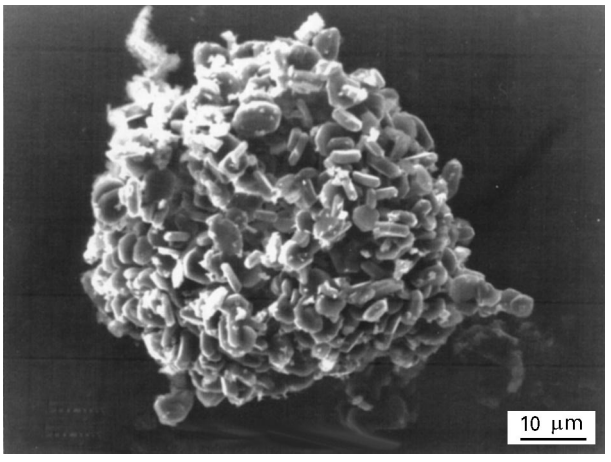

Figure 6 SEM micrograph of a particle of batch δ1000 after heating in chlorine atmosphere at 1000 °C during 40 h (run 19 in Table II, XRD diagram in Fig. 3d).

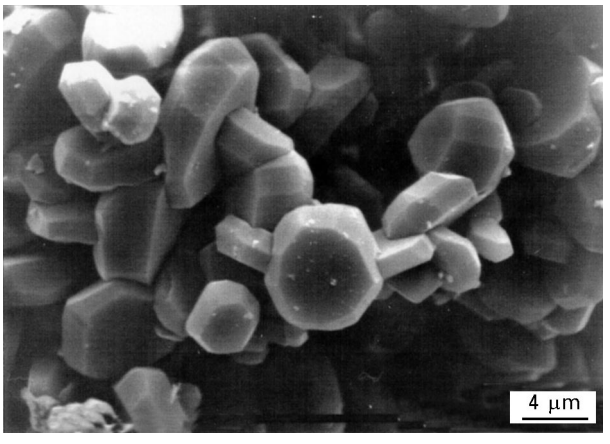

Figure 7 SEM micrograph of surface detail of particle of batch δ950 after heating in chlorine atmosphere at 950 °C during 30 h (run 12 in Table II, XRD diagram in Fig. 2d).

transformation sequence from well-crystallized boehmite. Therefore the formation of α-phase during the thermal treatments in air must involve a mechanism of solid state diffusion in which dehydration of OHs contained in transition aluminas favours the transformation. This process is consistent with the observed slow transformation kinetics in these treatments.

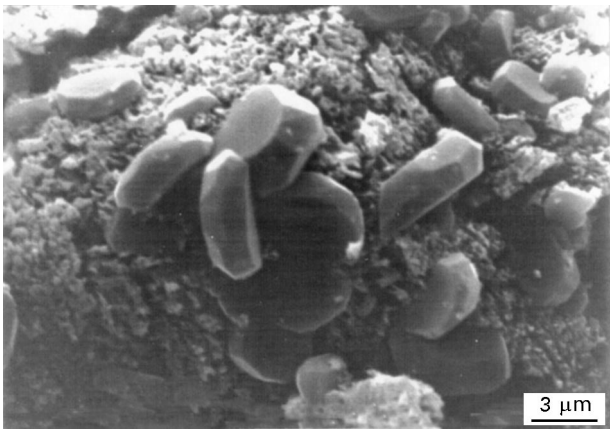

Figure 8 SEM micrograph of surface detail of a particle of batch δ950 after heating in chlorine atmosphere at 950 °C during 30 h (run 12 in Table II, XRD diagram in Fig. 2d).

Chlorine gas, due to its strong dehydrating behaviour, should enhance the transformation between transition aluminas in the same sequence as for treatments in air. However, this effect cannot be verified in long-term heatings because of the enhancing effect (compared to air) on α-phase formation at the expense of transition phases. The morphological changes observed after treatments in chlorine atmosphere, which are very different to those associated to air treatments, suggest that when chlorine is present an alternative mechanism, additional to the dehydration one, would give the main contribution to α-phase formation. In chlorinated samples, the observed crystals have the typical "barrel-shaped" habit of α-Al_2O_3 [20]. Thus, these crystals can be identified as belonging to α-phase and crystal growth must occur from a fluid phase [21], which in our case is the gaseous phase. We suppose that the transport from transition aluminas to α-phase was carried out by $AlCl_3$(g). Then, chlorine action can be interpreted as a two-step mechanism involving "dissolution" of transition aluminas in a vapour phase and further precipitation of the α-phase. This mechanism allows the direct transformation of each transition phase in the stable one and can be represented by the following equations

$$2\,(\delta, \theta)\text{-}Al_2O_3(s) + 6\,Cl_2(g) = 4\,AlCl_3(g) + 3\,O_2(g) \quad (1)$$

$$4\,AlCl_3(g) + 3\,O_2(g) = 2\,\alpha\text{-}Al_2O_3(s) + 6\,Cl_2(g) \quad (2)$$

Despite chlorination of aluminas is not thermodynamically favourable, from data [1] for reaction 2 and for 1.013×10^5 Pa of chlorine pressure, the equilibrium partial pressure of $AlCl_3$(g) is 60.78 Pa at 900 °C, 101.3 Pa at 950 °C and 182.3 Pa at 1000 °C. Even for these low $AlCl_3$(g) pressures, a vapour mass transport would be feasible [19]. Crystallization of α-Al_2O_3 will depend on the $AlCl_3$(g) saturation in vapour phase relative to the equilibrium values. Based on the high reactivity of transition aluminas [22], reaction 1 could be considered a suitable $AlCl_3$(g) supply to give a correct saturation. Because, for all chlorine runs, the same size of α-Al_2O_3 crystals was observed, a nearly

equilibrium growth can be supposed. In the following, the ability of reaction 1 to "dissolve" transition aluminas and the efficiency of reaction 2 to produce α-Al_2O_3 crystallization will be discussed in the light of OH presence.

The formation of $AlCl_3$ through reaction 1 would be assisted by OH. In the dehydration process through the Cl_2–OH interaction, chlorine molecules could be dissociated and HCl(g) and Cl(g) could be produced. Chlorine atoms, which have greater chemical activity than chlorine molecules, would be more effective to form $AlCl_3$(g).

Regarding α-Al_2O_3 crystallization, in chemical vapour deposition studies about alumina films from $AlCl_3$(g) precursor, the influence of oxygen donor from the systems H_2O–$AlCl_3$ [23], CO_2–H_2–$AlCl_3$ [23, 24], O_2–$AlCl_3$ [23] has been reported. Although all these systems are thermodynamically favourable, from the point of view of their kinetics O_2 is the least effective as oxygen donor, whereas the H_2O–$AlCl_3$ system is the most effective [23]. A study on the growth of α-Al_2O_3 from fluorinated γ-Al_2O_3 in presence of water vapour [25] shows the development of hexagonal platelets, very similar to the crystals shown in the present work. The authors explain their observations based on the crystallization of α-Al_2O_3 from AlF_3(g) + H_2O(g) reaction. In our case, the formation of water vapour from thermal dehydration of OH that did not react with chlorine could assist stable phase crystallization by the following reaction

$$2\,AlCl_3(g) + 3\,H_2O(g) = \alpha\text{-}Al_2O_3(s) + 6\,HCl(g) \quad (3)$$

In our closed system, the initial concentration of reactants and the OH content in transition aluminas would determine which reaction (2 or 3) produces the stable phase crystallization. However, it was not the aim of the present work to investigate their relative contribution.

5. Conclusion

The following conceptual scheme represents all process that would describe transformation of transition aluminas to the α-Al_2O_3 phase in air and in chlorine atmospheres

$$\begin{array}{ccccc} 2\,\delta\text{-}Al_2O_3(s) & \rightarrow & 2\theta\text{-}Al_2O_3(s) & \rightarrow & 2\alpha\text{-}Al_2O_3(s) \\ + & & + & & \\ 6\,Cl_2(g) & & 6\,Cl_2(g) & & \end{array}$$

$$\begin{array}{lll} \searrow & & \searrow \\ \rightarrow & \rightarrow & 4\,AlCl_3(g) + 3\,O_2(g) \rightarrow 2\,\alpha\text{-}Al_2O_3(s) + 6\,Cl_2(g) \\ & & 4\,AlCl_3(g) + 6\,H_2O(g) \rightarrow 2\,\alpha\,Al_2O_3(g) + 12\,HCl(g) \end{array}$$

Thermal treatments in air atmosphere allow the subsequent transformation throughout transition aluminas to α-phase. In chlorine atmosphere, an alternative path that involves the direct transformation of each transition phase by vapour transport through $AlCl_3$(g) is evidenced. In this scheme the OH presence in transition aluminas would enhance the $AlCl_3$(g) formation and either oxygen as in reaction 2 or water vapour as in reaction 3 could favour α-Al_2O_3 crystallization. For higher temperatures, it was found that both the relative amount of stable phase and the number of crystals increase. Then, it can be inferred that the higher the temperature the greater the maximum number of nuclei formed over which, at equilibrium, a maximum final growth through $AlCl_3$(g) is achieved. A greater number of nuclei could be present in starting batches prepared at higher temperatures, as can be supposed from the observation of slight production of α-phase in the starting batch δ1000.

Acknowledgements

We thank Silvia M. Dutrús and Carlos N. Cotaro of the Sección Caracterización de Materiales of Centro Atómico Bariloche for SEM micrographs.

References

1. M. W. CHASE Jr., C. A. DAVIES, J. R. DOWNEY Jr., D. J. FRURIP, R. A. McDONALD and A. N. SYVERUD, *J. Phys. Chem. Ref. Data.* **14** (1985).
2. K. WEFERS and C. MISRA, ALCOA Technical Paper N° 19, Revised, Aluminum Company of America (1987).
3. S. J. WILSON, *J. Solid State Chem.* **30** (1979) 247.
4. Z. D. ZIVKOVIC, *Thermochim. Acta* **21** (1977) 391.
5. R. A. SHELLEMAN and G. L. MESSING, *J. Amer. Ceram. Soc.* **71** (1988) 317.
6. E. K. BEAUCHAMP and M. J. CARR, *ibid.* **73** (1992) 49.
7. L. A. XUE and I. W. CHEN, *J. Mater. Sci. Lett.* **11** (1992) 443.
8. B. C. LIPPENS and J. H. de BOER, *Acta Crystallogr.* **17** (1964) 1312.
9. R. S. ZHOU and R. SNYDER, *ibid.* **B47** (1991) 617.
10. M. PIJOLAT, M. DAUZAT and M. SOUSTELLE, *Thermochim. Acta* **122** (1987) 71.
11. *Idem., Solid State Ionics* **50** (1992) 31.
12. P. BURTIN, J. P. BRUNELLE, M. PIJOLAT and M. SOUSTELLE, *Appl. Catal.* **34** (1987) 239.
13. G. C. BYE and G. T. SIMPKIN, *J. Amer. Ceram. Soc.* **57** (1974) 367.
14. H. SCHAPER, D. J. AMESZ, E. B. M. DOESBURG and L. L. VAN REIJNEN, *Appl. Catal.* **9** (1984) 129.
15. H. SCHAPER, E. B. M. DOESBURG, P. H. M. DE KORTE and L. L. VAN REIJEN, *Solid State Ionics* **16** (1985) 261.
16. M. DAUZAT, M. PIJOLAT and M. SOUSTELLE, *J. Chimie Physique* **85** (1988) 865.
17. E. M. LOPASSO, J. M. ASTIGUETA, J. J. ANDRADE GAMBOA and D. M. PASQUEVICH, in Proceedings of the 49th International Congress on Metallurgy and Materials Technology (50 Anniversary of ABM) San Pablo, Brasil, **IX** (October, 1994) p. 341.
18. D. M. PASQUEVICH, F. LOVEY and A. CANEIRO, *J. Amer. Ceram. Soc.* **72** (1989) 1664.

19. J. J. ANDRADE GAMBOA and D. M. PASQUEVICH, *ibid.* **75** (1992) 2934.
20. L. G. BERRY and G. MASON, "Mineralogy: concepts, descriptions, determinations" (W. H. Freeman and Company, San Francisco and London, 1959).
21. B. R. PAMPLIN (ed.), "Crystal Growth", International Series on the Science of the Solid State, Vol. **16,** 2nd edn (Pergamon Press, Oxford, 1980).
22. I. S. PAP, G. MINK, I. BERTÓTI, B. ZELEI and T. SZÉKELY, *Thermochim. Acta* **149** (1989) 205.
23. P. WONG and McD. ROBINSON, *J. Amer. Ceram. Soc.* **53** (1970) 617.
24. S. W. CHOI, C. KIM, J. G. KIM and J. S. CHUN, *J. Mater. Sci.* **22** (1987) 1051.
25. C. A. SHAKLEE and G. L. MESSING, *J. Amer. Ceram. Soc.* **77** (1994) 2977.

Received 21 August 1995
and accepted 13 November 1996